



Changes in Soil Properties over Time after a Wildfire and Implications to Slope Stability

Idil Deniz Akin, A.M.ASCE¹; Taiwo O. Akinleye, S.M.ASCE²; and Peter R. Robichaud, M.ASCE³

Abstract: Postwildfire forests are dynamic environments. Wetting-induced shallow landslides are observed at varying times after wildfires, but the reasons are not fully known. This study investigates the time-dependent changes in soil properties and mechanical and hydrologic soil behavior of hillslopes after the 2019 Williams Flats Wildfire near Keller, WA and demonstrates the implications of these changes to slope stability. Soil water repellency, organic content, fine content, soil water retention curve, hydraulic conductivity, friction angle, and in-situ suction-saturation data provides initial evidence that soil properties fluctuate over a year after the wildfire. The results therefore suggest that soil properties that are measured immediately after the wildfire are misleading for long-term slope stability analysis. The stability of a steep (45°) slope is found to be most affected by the fluctuations in friction angle and soil water retention over the year. The comparison of suction-saturation response near a burned and unburned location demonstrates the effects of macropores that are formed after the wildfire and evapotranspiration on slope stability. The hillslope stability at the unburned location reduces rapidly in April upon snowmelt, whereas the stability at the burned location, which has macropores, shows the rapid decrease in late-January, with the onset of snowfall. **DOI: 10.1061/JGGEFK.GTENG-11348.** © 2023 American Society of Civil Engineers.

Introduction

The Western United States experiences large wildfires every summer, which have been increasing in both size and frequency in recent decades (Westerling et al. 2006; Dennison et al. 2014; Westerling 2016). The projected increase in summer droughts and global temperature is expected to increase the magnitude and severity of wildfires (Masson-Delmotte et al. 2021). Wildfires are multiscale, multidisciplinary problems that have both primary (or direct) and secondary (or indirect) effects. Landslides during wet seasons following wildfires and corresponding flood hazards are among the "cascading and often unacknowledged" secondary effects of wildfires (Abatzoglou et al. 2014; Smith et al. 2016). However, research on postwildfire landslides is limited, and the landslide trigger mechanisms are not explained in a complete framework (Parise and Cannon 2012). Identifying a wildfire event as the trigger of a landslide is challenging because, while landslides can occur as early as during the first rainy season after the fire, they can also occur months or even years after the fire (e.g., Wondzell and King 2003). The timedependent changes on soil properties after a wildfire and implications to hillslope stability are unknown.

Postwildfire slope stability is a global concern because instability issues (i.e., erosion and wetting-induced shallow landslides) can (1) cause direct downstream damage as hillslope material moves into

Note. This manuscript was submitted on September 20, 2022; approved on February 13, 2023; published online on April 24, 2023. Discussion period open until September 24, 2023; separate discussions must be submitted for individual papers. This paper is part of the *Journal of Geotechnical and Geoenvironmental Engineering*, © ASCE, ISSN 1090-0241.

streams, transportation corridors, or settlements; or (2) trigger catastrophic debris flows and be a serious threat to human life, ecosystems, and infrastructure. So far, post-wildfire slope stability research has mainly been focused on analyzing (1) erosion (e.g., Robichaud et al. 2000; Parise and Cannon 2012); or (2) debris flow initiation through empirical, empirically based probabilistic, or statistical models that use historical data (e.g., Gartner et al. 2008, 2014; Cannon et al. 2010; Staley et al. 2013, 2016, 2017). Few studies on postwildfire shallow landslides have identified the main landslide trigger mechanisms as loss of structural support from roots (i.e., root cohesion) or rises in positive pore water pressures with the rise of the water table after a wetting event (e.g., Meyer et al. 2001; Cannon and Gartner 2005; Wondzell and King 2003; Schmidt et al. 2001; De Graff 2018). Few researchers have observed an increase in soil saturation in field measurements or identified increased saturation due to reduced transpiration rates as a potential landslide trigger mechanism (e.g., Megahan 1983; Cannon et al. 2001; Swanson 1981). Wetting-induced shallow landslide mechanisms and the effect of roots on slope stability, independent of wildfires, have been studied for decades. The mechanisms of wetting-induced shallow landslides have been identified as increases in positive pore water pressures with a rise of the water table and decreases in negative pore water pressures (or matric suction) with the advancement of a wetting front without a rise of the water table (e.g., Fourie et al. 1999; Collins and Znidarcic 2004; Sidle and Ochiai 2006; Muntohar and Liao 2008; Godt et al. 2009; Lee et al. 2009). The effect of roots on slope stability has been identified in controlled studies as an increase in stability due to structural support and matric suction around the roots (e.g., Wu et al. 1995; Gray and Sotir 1996; Ng et al. 2016; Oorthuis et al. 2018). However, the suction-saturation response of wildfire-burnt slopes and corresponding effects on slope stability have not been investigated.

This study presents the changes in soil properties, suctionsaturation response of the slope, and corresponding slope stability over time after the 2019 Williams Flats wildfire in Colville Indian Reservation, near Keller WA. An extensive laboratory and field work to measure soil water repellency, organic content, friction angle, hydraulic conductivity, soil water retention curve was

¹Associate Professor, Dept. of Civil, Construction, and Environmental Engineering, North Carolina State Univ., Raleigh, NC 27695 (corresponding author). ORCID: https://orcid.org/0000-0002-1946-4951. Email: idakin@ncsu.edu

²Graduate Student, Dept. of Civil and Environmental Engineering, Washington State Univ., Pullman, WA 99164. ORCID: https://orcid.org/0000-0002-1374-3562

³Research Engineer, Forest Service, US Department of Agriculture, Rocky Mountain Research Station, Moscow, ID 83843. ORCID: https://orcid.org/0000-0002-2902-2401

complemented with field data from suction and water content sensors to quantify the changes. A hypothetical steep slope was used to demonstrate the implications to hillslope stability. The time-dependent changes in model input parameters and effects on slope stability calculation were presented.

Field Work

Study Site

The study site was selected after the 2019 Williams Flats Fire in Colville Indian Reservation near Keller, WA (Akin and Akinleye 2021) from an intersection between a high-burn severity area and moderately-burn severity area as defined by Parsons et al. (2010). Burn severity map of the site (Fig. 1) was generated using Landsat 8 OLI satellite imageries from data produced under the monitoring trends in burn severity (MTBS) program jointly implemented USGS Earth Resources Observation and Science Center and the United States Forest Service (USFS) Geospatial Technology and Applications Center (GTAC). This program provided computed information on fire occurrence locations based on data made available

by federal and state agencies, and other reliable resources. The burnt vegetation was primarily ponderosa pine (*Pinus ponderosa*) and mixed conifer. In addition, light logging slash, different brush, and grass species, including antelope bitterbrush (*Purshia tridentata*) and *Ceanothus*, and seasonal wildflowers comprised the vegetation at the site.

The fire was contained on August 25, 2019, and the first field visit took place on October 2, 2019. Two trees and surrounding areas of 2-m radii were selected for field instrumentation and sample collection [Fig. 2(a)]. The first area is next to a burned tree from a high burn severity area and will be referred as the dead tree location. The vegetation in this area was charred and wildfire ash was apparent on the soil surface in October 2019. In addition, this site consisted of macropores generated by burned roots [Fig. 2(b)]. The second location is next to an unburned tree from a moderately-burned area that is 300 m away from the dead tree location and will be referred as live tree. This area showed little or no evidence of vegetation or soil burn, and this was used as a baseline for comparison on the time-dependent changes in soil properties and influence of evapotranspiration on the suction-saturation response of the site.

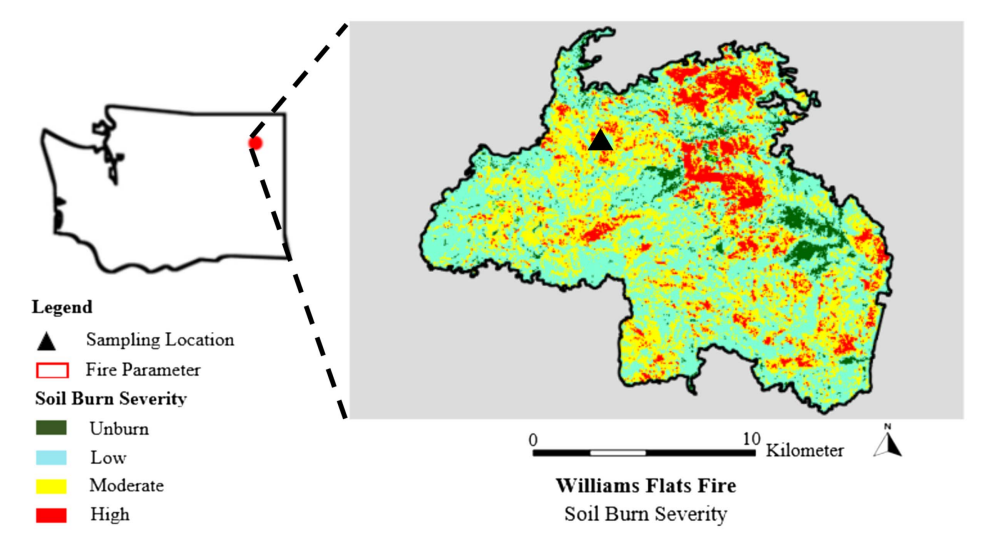


Fig. 1. Burn severity map of the site. [Map courtesy of MTBS (Monitoring Trends in Burn Severity).]

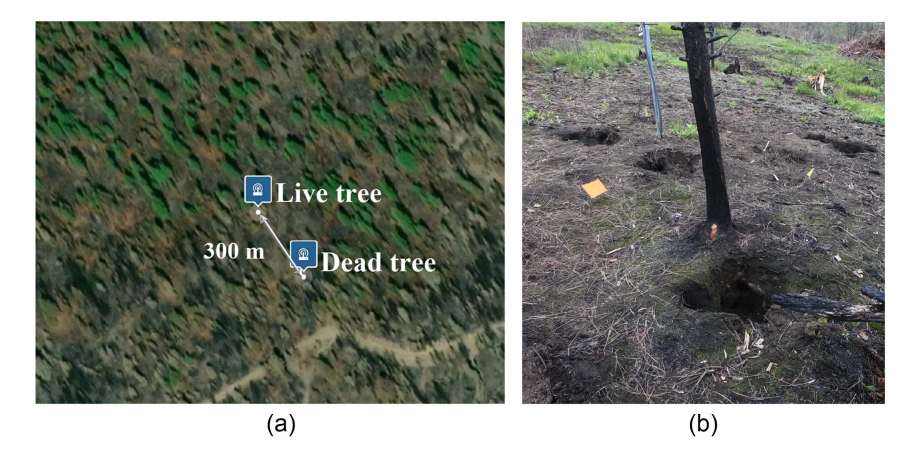


Fig. 2. (a) Sampling areas at the dead tree and live tree locations (image from ZENTRA Cloud, data sources © Mapbox © OpenStreetMap Improve this map © Maxar); and (b) macropores at the dead tree location.

Field Instrumentation

Soil water potential sensors with 2,000 kPa capacity (TEROS 21) and water content sensors (TEROS 11) were installed in October 2019 at three different depths (0.3, 0.5, and 1 m) in both locations, 2 m away from the trees. In addition, a standalone tipping bucket rain gauge was installed in May 2020 between the dead tree and live tree locations.

A hand auger was used to drill 1.2-m-deep boreholes and the water content sensors were placed horizontally using the sensor installation tool. The TEROS 21 sensor consists of two fixed porous ceramic discs that are separated by a printed electric circuit board that forms a capacitor and a thermistor is located underneath the sensor that measures temperature. The ceramic discs are poor conductors of electric current and when placed in contact with soil, the water content and suction attain equilibrium with that of the soil after an elapsed time. The sensor then measures the water content of the ceramic discs and is translated into matric suction based on a predetermined relationship between water content and matric suction of the ceramic discs. To ensure good contact between the ceramic disks and surrounding soil, the soil that was removed from the borehole at each sensor depth was first packed near field density around the suction sensors in plastic cups that were used as molds. Then the soil blocks where the sensors were embedded were extracted from the cups and placed in the boreholes. For each set of sensors, a ZL6 data logger with a capacity of 6 sensors was used for automated data acquisition. The sensors, sensor installation tool, and data loggers were obtained from Meter Group, Pullman WA. The TEROS 11 sensor at live tree location at 1 m depth was replaced with a TEROS 12 sensor in July 2020, after a bear attack. TEROS 12 water content sensor is identical to TEROS 11 but has an additional electrical conductivity sensor.

Sample Collection and Field Measurements

Bulk and intact samples were collected to a depth of 2.2 m to identify the soil profile and perform the standard soil classification tests. Bulk samples were collected with a hand auger and intact samples were collected using 0.15-m-long thin-walled samplers. Additional intact and bulk samples were collected in subsequent field visits in November 2019, May 2020, June 2020, July 2020, August 2020, and September 2020 from the surface and from a depth of 0.5 m to perform the laboratory experiments. 0.5 m was selected to avoid the top layer with high organic content as a representative depth to determine the soil properties that are necessary for slope stability analysis or modeling (i.e., friction angle, hydraulic conductivity, soil water retention curve). The organic content, fine content, and soil water repellency of the surface soil was measured both for 0.5 m soil and surface soil to understand the trends in hydraulic conductivity. In each visit, a 0.5-m trench was dug, sample collection and field measurements were performed, the trench was closed and flagged to avoid double-sampling from the same location in the following visits. 8-cm-diameter and 5-cm-height thin-walled sampling rings were used to collect intact samples for water droplet penetration time (WDPT) tests. 6.3-cm-diameter and 2.5-cm-height sampling rings were used to collect intact samples for direct shear test. Bulk soil was collected to perform loss on ignition, water retention curve (with WP4C), and standard soil classification tests.

Laboratory Experiments

Water droplet penetration time (WDPT) tests (Van't Woudt 1959) were performed with 16 equally-spaced deionized water droplets as explained in Akin and Akinleye (2021). The water repellency was

classified based on the average time required for the droplets to be absorbed in the soil, according to King (1981) and Chenu et al. (2000).

Loss on ignition (LOI) test was performed as described in Scalia et al. (2014). Oven-dried (105°C) soil samples were kept in a furnace (550°C) for 4 h. The mass difference before and after the furnace was used to calculate LOI and related to soil organic content.

The soil water retention curves were measured in the laboratory using a chilled-mirror dew point technique (WP4C, Meter Group, Pullman WA) as described in Akin and Akinleye (2021). Oven-dried (105°C) bulk soil was mixed with deionized water to achieve target degree of saturations (between 0.1 and 0.8) and compacted in steel WP4C cups at a constant void ratio of 0.57. The cups were sealed with plastic caps after compaction for 24 h and suction measurements were taken. Saturation of the samples were calculated from gravimetric water content measured after suction measurements.

For the direct shear tests, intact samples were carefully extracted and placed in the shear box. A stepper-motor controlled load frame was used to apply shear at a constant displacement rate of 0.5 mm/min.

Slope Stability Analysis

The general form of the infinite slope stability equation is given (e.g., Lambe and Whitman 1969; Cho and Lee 2002) as

$$FS = \frac{\tau_f}{\tau_m} = \frac{c' + \cos^2\beta [q_0 + \gamma H_{wt} + (\gamma_{sat} - \gamma_w) z_w] \tan \phi'}{\sin\beta \cos\beta [q_0 + \gamma H_{wt} + \gamma_{sat} z_w]}$$
(1)

where FS = factor of safety; c' = soil cohesion; β = slope angle; q_0 = vegetation surcharge; H_{wt} = vertical depth of the water table from the ground surface; z_w = vertical depth to the failure surface from the water table; ϕ' = effective friction angle; γ = total unit weight; γ_{sat} = saturated unit weight; and γ_w = unit weight of water.

A modified form of Eq. (1) was used in this study for slope stability analysis [Eq. (2)], following the suction stress concept (Lu and Likos 2006; Lu and Godt 2008)

$$FS(z_u) = \frac{\tan \phi'}{\tan \beta} + \frac{2c_r}{\gamma(H_{wt} - z_u)\sin 2\beta} - \frac{\sigma^s}{\gamma(H_{wt} - z_u)} (\tan \beta + \cot \beta) \tan \phi'$$
 (2)

where z_u = depth from the water table in the unsaturated zone. Here suction stress includes the contribution of cementation and interparticle forces as due to water retention (i.e., adsorptive interparticle forces, σ_a^s and capillary interparticle forces, σ_c^s) and defined by Akin and Likos (2020) as:

$$\sigma^{s}(\psi) = \sigma_{a}^{s}(\psi) + \sigma_{c}^{s}(\psi) \tag{3a}$$

$$\sigma_a^s = \left(\frac{\psi}{10^6}\right) \times \sigma_{dry}^s \tag{3b}$$

$$\sigma_c^s = \left(\frac{\psi_{ae}}{\psi_{ae} + \psi}\right) \times \psi \times \left(\frac{S_e}{S_{e,ae}}\right) \tag{3c}$$

where σ_{dry}^s = suction stress at oven-dry (105°C) conditions; 10⁶ = theoretical maximum suction (kPa); ψ is suction; S_e = effective saturation; ψ_{ae} = air entry pressure (which was equated to the inverse of α); and $S_{e,ae}$ = effective saturation at air entry pressure. The model requires an experimental measurement of suction stress at dry conditions, which can be measured with Brazilian tensile

strength test (Akin and Likos 2017a, b) among other methods, and the remaining scaling parameters are from SWRC. Both ψ_{ae} and $S_{e,ae}$ are determined using the Van Genuchten (1980) model as

$$S_e = \frac{S - S_r}{1 - S_r} = \left[\frac{1}{1 + (\alpha \psi)^n}\right]^{(1 - 1/n)}$$
 (4)

where S = saturation; $S_r =$ residual saturation; and α and n = fitting parameters.

A hypothetical steep slope (45°) was used for slope stability analysis. Two FS analyses were conducted. The first analysis, which will be referred as constant soil properties analysis, used the minimum friction angle measured over the year (27.1°) and constant SWRC parameters ($\alpha=0.008$, n=1.4, $S_r=0.0004$), with the goal of demonstrating only the effect of suction-saturation response of wildfire-burnt soil on slope stability. In the second analysis, which will be referred as monthly analysis, the input parameters of Eq. (2) were altered based on field measurements. October 2019 soil parameters were used until November 2019, November 2019 parameters were used until the end of March 2020, May 2020 parameters were used from April to June 2020, June 2020 parameters were used until July 2020. August 2020 parameters were used from August 2020 until the end of October 2020.

Results

Soil Properties

The initial soil properties at the dead tree location measured with October 2019 soil samples showed that fine content was 47% at the surface, 31% at 0.5 m, and 10% at 1.2 m depth. The organic content was 9.3% at the surface, 2.8% at 0.5 m, and 1.3% at 1.2 m. The void ratio was 1.57 at the surface and 0.57 at 0.5-m depth.

The soil properties changed over time both at the surface and at 0.5 m depth. The water repellency of the surface soil (Fig. 3) fluctuated from slightly-repellent in November 2019, May 2020, and August 2020 to strongly repellent in July 2020. The 0.5-m soil showed nonrepellent behavior over the year except for occasional local slightly repellent spots detected in July 2020.

Soil organic content (Fig. 4) ranged between 3.4% and 9.5% for the surface soil whereas stayed relatively constant between 2.4% and 3.7% for the 0.5-m soil. The most drastic changes for the surface soil were the steep reduction from October 2019 (9.3%) to

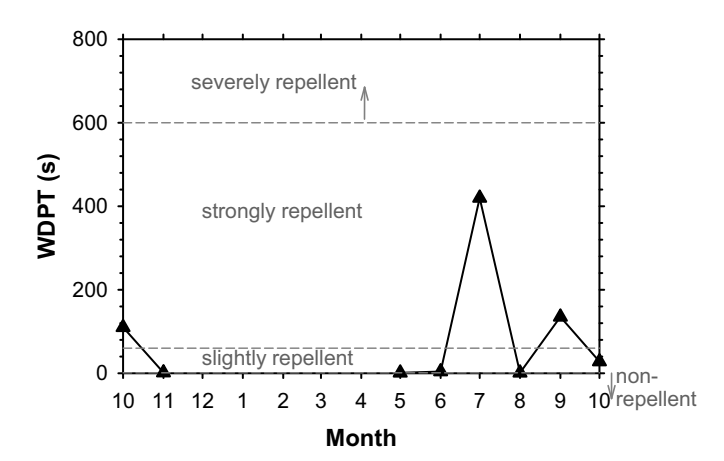


Fig. 3. Water repellency of surface soil at the dead tree location over the year.

November 2019 (3.4%) and steep increase from August 2020 (6.6%) to September 2020 (9.5%).

The fine content (Fig. 5) of the surface soil stayed relatively constant at around 45%, except for August 2020 (33%) and September 2020 (38%), whereas for 0.5-m soil, fine content increased over time from 31% in October 2019 to a maximum of 53% in May 2020. The increase was primarily because of an increase in clay content. The clay content was 6% in October 2019 and reached a maximum of 17% in May 2020. For the surface soil, clay content fluctuated between 6% and 10%, with no apparent trend over the year.

The saturated hydraulic conductivity fluctuated by two orders of magnitude for the surface soil and an order of magnitude for the 0.5-m soil over the year (Fig. 6). A prominent difference (i.e., order of magnitude difference) in hydraulic conductivity between the two depths was measured only in November 2019, May 2020, and October 2020. The minimum and maximum hydraulic conductivity were measured in May 2020 (minimum) and August 2020 (maximum).

The friction angle of the 0.5-m soil gradually decreased from 38.1° in October 2019 to a minimum of 27.1° in June 2020 (Fig. 7). After the minimum is reached, the friction angle gradually increased and reached 37.9° in August 2020.

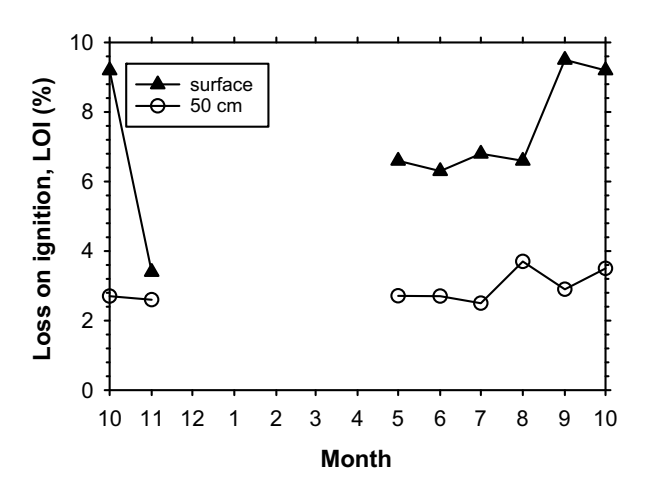


Fig. 4. Soil organic content of the surface and 0.5 m soil at the dead tree location over the year.

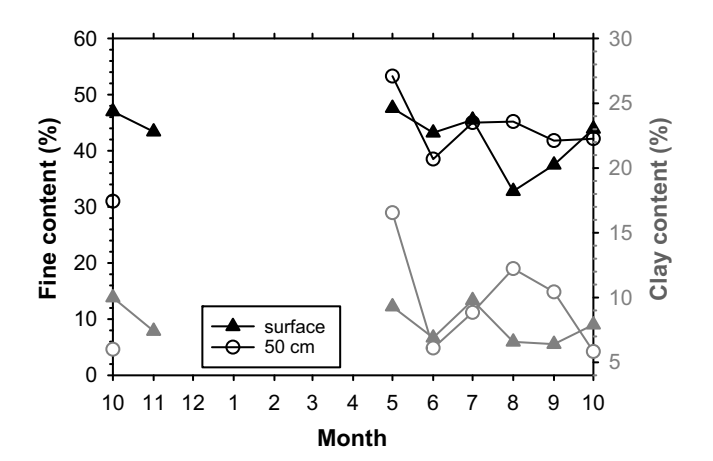


Fig. 5. Fine content and clay content of the surface and 0.5 m soil at the dead tree location over the year.

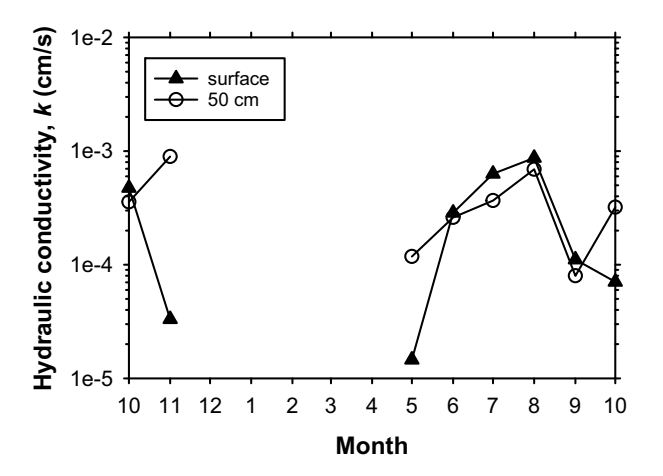


Fig. 6. Saturated hydraulic conductivity of the surface and 0.5 m soil at the dead tree location over the year.

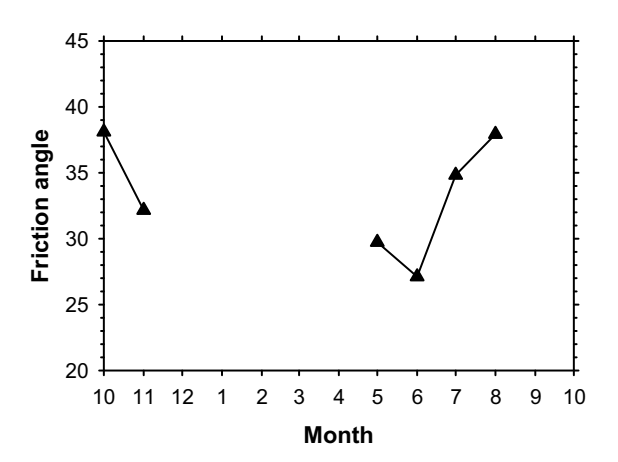


Fig. 7. Friction angle of the 0.5 m soil at the dead tree location over the year.

The SWRC of the 0.5-m soil measured in the laboratory varied each month. The Van Genuchten (1980) effective saturation-based best-fit curves are shown for clarity (Fig. 8). The November soil maintained the lowest suctions over the entire saturation range. This was followed by September 2020, August 2020, October 2019, July 2020, October 2020, and May 2020 soils.

Sensor Data and Hillslope Stability

Limited rainfall data was recorded over the year (Fig. 9). The delay in installation of the rain gauge and the region being snowmelt-dependent rather than rainfall-dependent limited the hydrology data. Major storm events are seen in June 2020 and October 2020, resulting in a cumulative rainfall of 160 mm by the end of the first year after the wildfire.

The suction and saturation trends in 0.3, 0.5, and 1 m and corresponding factor of safety of the hypothetical slope calculated with the constant soil properties are shown in Fig. 10. The complete data set is published in Akin (2023). The gaps in data in summer 2020 are due to two bear attacks that took down the data loggers or unplugged the sensors from the loggers. In all three depths, the live tree generally maintained higher suctions and lower saturations than the dead tree. At the live tree location, a distinct reduction in suction that corresponds to a rapid increase in saturation was observed in early April 2020 in all three depths. A second distinct

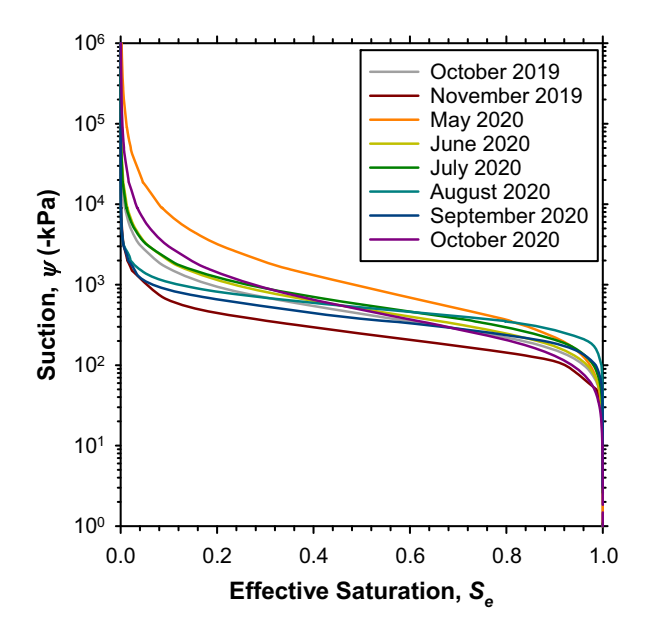


Fig. 8. Soil water retention curve of the 0.5-m soil at the dead tree location over the year.

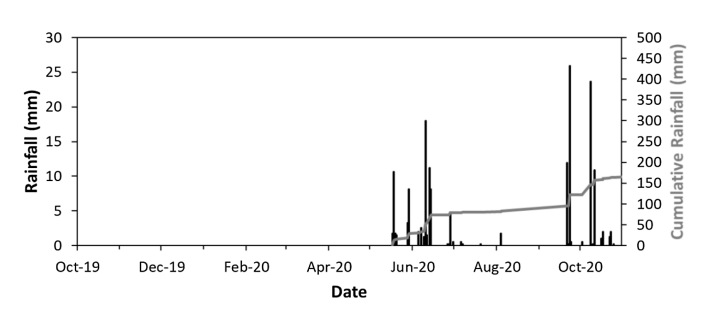


Fig. 9. Rainfall data

increase in saturation and corresponding decrease in suction were seen earlier, in mid to late October 2019 at 0.3 and 0.5 m. Conversely, in mid-June to early July, a distinct increasing trend in suction that is paired with a gradual decreasing trend in saturation was observed at all three depths. At the dead tree location, at 0.5 m, a sharp increase in saturation that coincided with a decrease in suction was in mid- to late-October, at the same time as the live tree location. After that, the first rapid increase in saturation that corresponded to a rapid decrease in suction was observed in mid-to late-December. From that point on, the saturation kept increasing incrementally, until nearly saturated state was achieved in April 2020.

The factor of safety analysis at 0.5 m depth showed an initial increase in FS at both locations, followed by a sharp decrease in late October 2019. After that, at the live tree location FS remained constant at around 1.7 until a rapid decrease to 1.4 in April 2020. At the dead tree location, the first reduction in FS was from 2.1 to 1.8 in late December 2019, followed by a distinct reduction to 1.3 in late January, eventually reaching close to 1 in June 2020.

Discussion

Soil Properties over Time

The WDPT results showed that water repellency is not specific to immediately after the wildfire, but water-repellent conditions can

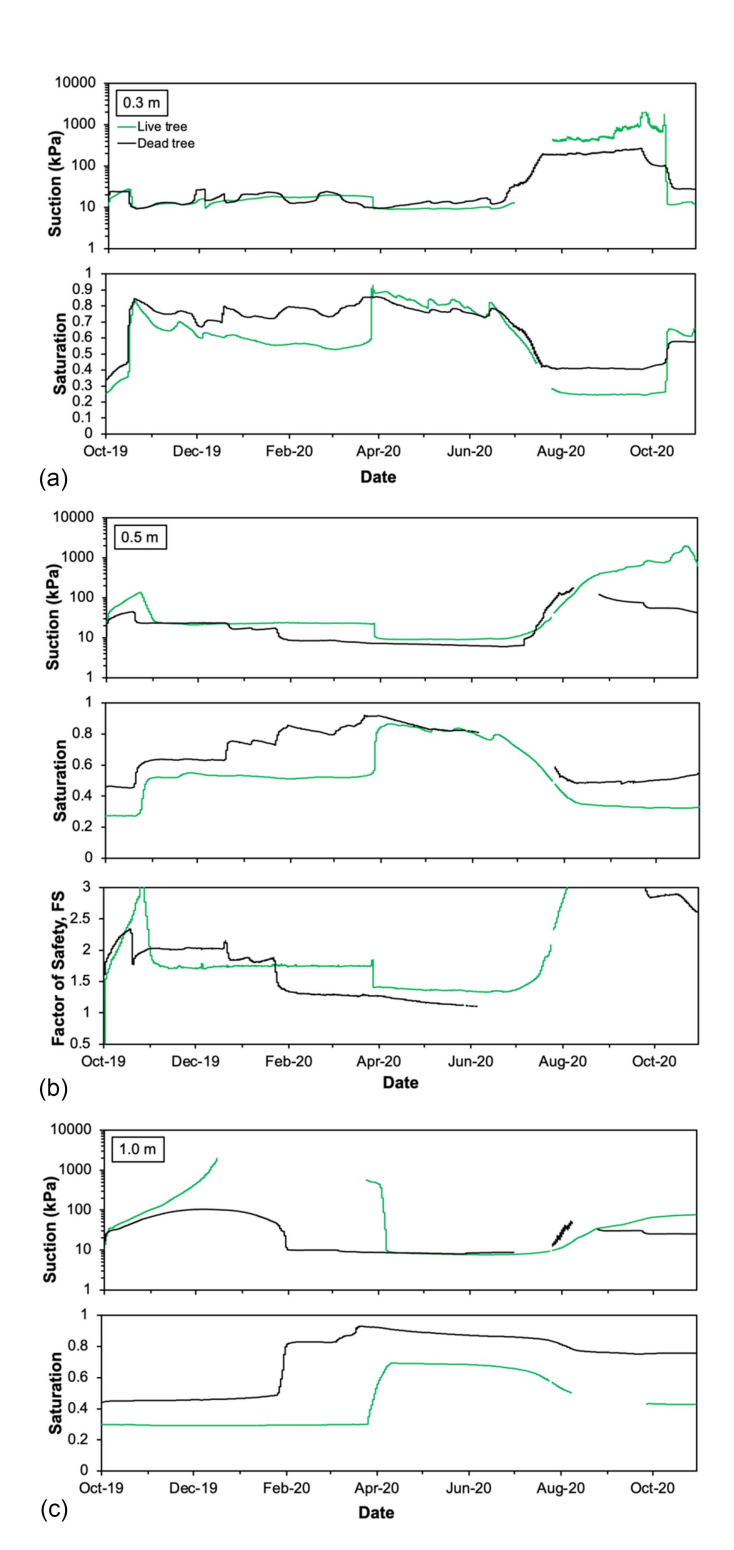


Fig. 10. Suction and saturation data from the field sensors for (a) 0.3 m; (b) 0.5 m; and (c) 1 m soil. The factor of safety of a 45° slope calculated using 0.5 m data is also shown in (b).

be observed and change over time after the fire. Soil water repellency is associated with organics, but no apparent trend was observed between the LOI and WDPT data because measured repellency values are reported as actual water repellency rather than potential water repellency, which incorporates the effect of water content in addition to organics (e.g., Dekker et al. 2001; Doerr et al. 2000). Soil water repellency depends on water content, where hyperdry soils remain water repellent until water retention

mechanism transitions from adsorption to capillary condensation (e.g., Doerr and Thomas 2000). The hottest month July resulted in the most severe water repellency. To demonstrate the effect of water content, a second WDPT test was performed on the July 2020 surface sample, after the surface was wetted, and the average WDPT was found as 2 s. The potential contribution of seasonal wildflowers on soil organic matter was also discussed in Akin and Akinleye (2021), which resulted in an increase in organic content and water repellency in September 2020. An additional WDPT test was performed on the September 2020 surface soil collected from the live tree location, where a higher density of wildflowers was observed showed severely-repellent behavior with an average WDPT of over 20 min, demonstrating the contribution of organics on water repellency, independent of the wildfire.

The increase in fine content of 0.5 m soil in May 2020 to 53% is in the same line with the increase in clay content to 17%. The reduction in fine content of surface soil in August 2020 coincides with the increase in clay content in the 0.5-m soil. The temporal fluctuations in fine content at the surface and at 0.5 m depth indicate spatial variability or perturbation of the soil. To evaluate the variability, the fine contents of the surface soil and 0.5 m soil were also measured at the live tree location between May 2020 and October 2020. The fine content ranged between 37% and 44% for the surface soil and between 35% and 43% for the 0.5 m soil. Clay content in the live tree location ranged between 6% and 8% at the surface and 5% and 8% at 0.5 m depth. The more extreme fluctuations seen at the dead tree location indicates potential perturbation of soil. An apparent pathway for perturbation was through the macropores next to the sampling location. No animal burrows were observed in the site, but chipmunks and bears were present that could contribute with bioturbation.

The saturated hydraulic conductivity, k, showed an apparent trend with fine content, where an increase in fine content resulted in a decrease in k, as expected (e.g., Terzaghi and Peck 1967). At the surface, the maximum k (8.7 × 10⁻⁴ cm/s) was measured in August 2020, where fine content (32.8%) and clay content (6.6%) were minimum and conversely the minimum k (1.5 × 10⁻⁵ cm/s) was measured in May 2020, when fine content (47.6%) was the maximum. The influence of water repellency of the surface soil on k was not clearly observed. In July 2020, when the water repellency was the most severe, the k (6.3 × 10⁻⁴ cm/s) was close to the maximum k measured over the year, even though the fine content was 45.5%. Similarly, the other two months that showed strong water repellency, October 2019 and September 2020, did not show evidence of an influence on hydraulic conductivity.

The fluctuations in friction angle and SWRC are the most influential factors for a slope stability analysis. Particularly the 11° fluctuation in friction angle is critical for a slope stability analysis, although the reasons could not be explained fully. The fluctuations in the remaining soil properties do not correlate with the trend in friction angle over the year. The 0.5-m soil remained nonrepellent over the year. The organic content stayed in a narrow range and fluctuated between 2.4% and 3.7%. The only significant fluctuations seen in the 0.5-m soil was in fine content, which showed a minimum of 31% in October 2019 and a maximum of 53% in May; yet, the minimum friction angle was measured in June 2020, when fine content was 39%. The minimum friction angle was expected to be measured in May, when clay content was the highest (17%). Other potential factors that could affect friction angle includes seasonal changes in void ratio, presence of ash in soil in different concentrations, and presence of fine roots in the shearing plane, will be investigated in future studies.

For SWRC, the May 2020 soil maintaining higher suctions than the remaining 0.5-m soils particularly in mid- to high suction range

imply a high surface-active material (therefore high adsorptive water) or a material with small pores (therefore high capillary water) is present in the soil. This is reflected in fine content and clay content. The May soil has the maximum amount of fines (53%).

Temporal changes in soil properties are also seen in soils that are not affected by wildfires because of biological and structural macropores or seasonal precipitation (e.g., Das Gupta et al. 2006). For example, Zhao et al. (2021) found less than an order of magnitude decrease in the saturated hydraulic conductivity of 0.1-m and 0.2-m deep soil in the dry season in the Chinese Loess Plateau.

The results provided initial evidence that soil properties change over time after a wildfire. Whether these measured trends are because of spatial variability in soil properties, or they reflect the time-dependent changes in soil properties during the recovery of the forest requires more investigation. The spatial variability is expected to be minimal because of the sampling area confined within a 2-m radius. However, more data are required to reach a conclusion.

Post-Wildfire Slope Stability over Time

At all three locations, greater suctions and smaller saturations at the live tree location are attributed to evapotranspiration by the trees. The hydrology of the region is snowmelt-dominated, which is reflected in the sensor data. The snowmelt in April resulted in the most distinct jumps in saturation at the live tree location in all three depths. The constant parameter analysis for the 0.5 m soil showed the direct relationship between suction, saturation, and corresponding slope stability. At both locations, an increase in saturation corresponded to a decrease in suction and a decrease in factor of safety. The earlier onset of increase in saturation at the dead tree location resulted in a reduction in factor of safety four months earlier than what was observed in the live tree location. The gradual, stepwise increase in saturation at the dead tree location and the early onset of the increase was attributed to the presence of macropores at this location, which could facilitate snowmelt starting earlier than the surface.

The slope stability analysis was performed for the hypothetical steep slope, whereas the sensor data is from a mild slope. If the sensors were installed in a steeper slope, up to 30°, the sensors are expected to give the same output (e.g., Philip 1991). However, for even steeper slopes, the sensors are expected to measure lower water contents and higher suctions because of the reduced capillary effects. 45° angle was chosen to demonstrate a steep slope that gives factor of safety values approaching 1 in the wet season. Lower slope angles would show similar trends in factor of safety, but with higher magnitudes.

The nonuniform trends in post-fire soil properties have brought up two essential questions for a post-wildfire slope stability analysis in forest lands (1) can we rely on single measurements of soil properties; and (2) can single set of soil parameters measured at a certain time after the wildfire be used to model the stability over time?

The first question has been extensively addressed for slope stability analysis, even though not specifically for forest lands. Probabilistic models were developed to determine the probability of failure of the hillslopes rather than performing a deterministic factor of safety analysis (e.g., Hammond 1992). Such models consider the spatial variation of soil properties and uncertainties involved in field or laboratory testing (Cho 2007, 2010; Das et al. 2017; Griffiths and Fenton 2004; Hazra et al. 2017; Jha 2015; Jiang et al. 2015; Phoon et al. 2010). To address the second question, an additional FS analyses was conducted for the 0.5-m dead tree soil by keeping the October 2019 soil properties constant for the entire year and the results were compared with the monthly analysis

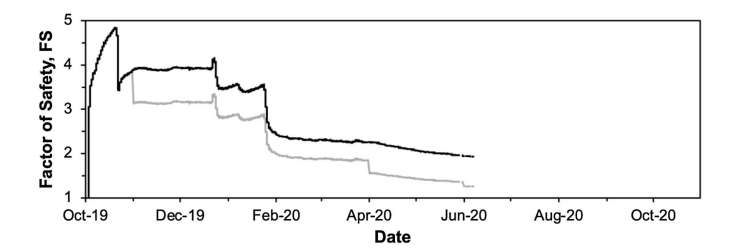


Fig. 11. Factor of safety calculated with monthly analysis (bottom) versus constant parameter analysis with October 2019 parameters (top) for the 0.5 m soil.

results (Fig. 11). The general trends remained the same; however, the factor of safety decreased throughout the year when monthly parameters were used. For example, in June 2020, the monthly analysis (gray) shows that the slope is approaching unstable conditions, whereas the constant parameter analysis (black), performed with October 2019 parameters, shows a stable slope with a factor of safety nearing 2.0. The results indicate that a slope stability analysis conducted with soil properties measured immediately after the wildfire may be misleading for long-term slope stability assessment.

Conclusions

The time dependent changes in soil properties after the 2019 Williams Flats wildfire and the implication to hillslope stability were evaluated over a one-year period through laboratory and in-situ measured soil hydrological and mechanical properties. The results gave initial evidence that soil properties both at the surface and at 0.5 m depth change over time after a wildfire. Soil water repellency, organic content, fine content, friction angle, hydraulic conductivity, and soil water retention behavior were measured over the year. The water repellency of the surface soil fluctuated from slightly repellent to strongly repellent. Soil organic content fluctuated between 3.4% and 9.5% for the surface soil and stayed constant between 2.4% and 3.7% for the 0.5-m soil. The fine content of 0.5-m soil increased from 31% in October 2019 to 53% in May 2020, indicated soil perturbation over time. The saturated hydraulic conductivity fluctuated by two orders of magnitude for the surface soil and an order of magnitude for the 0.5-m soil. The soil water retention curve measured each month was different. The friction angle fluctuated by 11° (between 38.1° and 27.1°) for the 0.5-m soil. The slope stability analysis performed on a 45° slope suggested that the soil properties measured immediately after the wildfire are not representative for long-term slope stability analysis. Field suction and water content sensors installed near a burned and an unburned tree demonstrated the effects of evapotranspiration and macropores (that were created from burnt roots) on hillslope stability. Sudden increases in pore water pressures upon snowmelt resulted in sudden reduction in slope stability near the unburned tree in April, whereas saturation gradually increased near the burned tree starting with snowfall in January, resulting a reduction in slope stability that could lead to unstable conditions four months before the live tree location.

Data Availability Statement

Some or all data, models, or code that supports the findings of this study are available from the corresponding author upon reasonable request.

Acknowledgments

This material is based upon work supported by the National Science Foundation (NSF) under Grant CMMI 1932129 (to IDA) and the US Department of Agriculture, Forest Service, Rocky Mountain Research Station (to PRR). We would like to thank Colville Indian Reservation for providing access to the site and Robert E. Brown for his help with field work.

References

- Abatzoglou, J. T., C. A. Kolden, J. F. C. DiMento, P. Doughman, and S. Nespor. 2014. "Climate-change effects, adaptation, and mitigation." In *Climate change: What it means for us, our children, and our grand-children*, edited by J. F. C. DiMento and P. Doughman, 53–104. Cambridge, MA: MIT Press.
- Akin, I. 2023. "Soil water retention over a year after the 2019 Williams flats wildfire." In *Proc.*, 2019 Williams Flats Wildfire Slope Stability. Gainesville, FL: DesignSafe-CI. https://doi.org/10.17603/ds2-zphj-na15.
- Akin, I. D., and T. O. Akinleye. 2021. "Water vapor sorption behavior of wildfire-burnt soil." *J. Geotech. Geoenviron. Eng.* 147 (11): 04021115. https://doi.org/10.1061/(ASCE)GT.1943-5606.0002648.
- Akin, I. D., and W. J. Likos. 2017a. "Brazilian tensile strength testing of compacted clay." *Geotech. Test. J.* 40 (4): 608–617. https://doi.org/10 .1520/gtj20160180.
- Akin, I. D., and W. J. Likos. 2017b. "Implications of surface hydration and capillary condensation for strength and stiffness of compacted clay." *J. Eng. Mech.* 143 (8): 04017054. https://doi.org/10.1061/(ASCE)EM .1943-7889.0001265.
- Akin, I. D., and W. J. Likos. 2020. "Suction stress of clay over a wide range of saturation." *Geotech. Geol. Eng.* 38 (1): 283–296. https://doi.org/10 .1007/s10706-019-01016-7.
- Cannon, S. H., and J. E. Gartner. 2005. "Wildfire-related debris flow from a hazards perspective." In *Debris-flow hazards and related phenomena*, 363–385. Berlin: Springer.
- Cannon, S. H., J. E. Gartner, M. G. Rupert, J. A. Michael, A. H. Rea, and C. Parrett. 2010. "Predicting the probability and volume of post wildfire debris flows in the intermountain western United States." *Bulletin* 122 (1–2): 127–144. https://doi.org/10.1130/b26459.1.
- Cannon, S. H., R. M. Kirkham, and M. Parise. 2001. "Wildfire-related debris-flow initiation processes, Storm King Mountain, Colorado." *Geomorphology* 39 (3–4): 171–188. https://doi.org/10.1016/S0169 -555X(00)00108-2.
- Chenu, C., Y. Le Bissonnais, and D. Arrouays. 2000. "Organic matter influence on clay wettability and soil aggregate stability." *Soil Sci. Soc. Am. J.* 64 (4): 1479–1486. https://doi.org/10.2136/sssaj2000.6441479x.
- Cho, S. E. 2007. "Effects of spatial variability of soil properties on slope stability." *Eng. Geol.* 92 (3–4): 97–109. https://doi.org/10.1016/j.enggeo.2007.03.006.
- Cho, S. E. 2010. "Probabilistic assessment of slope stability that considers the spatial variability of soil properties." *J. Geotech. Geoenviron. Eng.* 136 (7): 975–984. https://doi.org/10.1061/(ASCE)GT.1943-5606 .0000309.
- Cho, S. E., and S. R. Lee. 2002. "Evaluation of surficial stability for homogeneous slopes considering rainfall characteristics." *J. Geotech. Geoenviron. Eng.* 128 (9): 756–763. https://doi.org/10.1061/(ASCE)1090-0241(2002)128:9(756).
- Collins, B. D., and D. Znidarcic. 2004. "Stability analyses of rainfall induced landslides." *J. Geotech. Geoenviron. Eng.* 130 (4): 362–372. https://doi.org/10.1061/(ASCE)1090-0241(2004)130:4(362).
- Das, G. K., B. Hazra, A. Garg, C. W. W. Ng, N. Avani, and H. Lateh. 2017. "Bivariate probabilistic modelling of hydro-mechanical properties of vegetative covers." Adv. Civ. Eng. Mater. 6 (1): 235–257. https://doi.org/10.1520/acem20160049.
- Das Gupta, S., B. P. Mohanty, and J. M. Köhne. 2006. "Soil hydraulic conductivities and their spatial and temporal variations in a vertisol." *Soil Sci. Soc. Am. J.* 70 (6): 1872–1881. https://doi.org/10.2136/sssaj 2006.0201.

- De Graff, J. V. 2018. "A rationale for effective post-fire debris flow mitigation within forested terrain." *Geoenviron. Disasters* 5 (1): 1–9. https://doi.org/10.1186/s40677-018-0099-z.
- Dekker, L. W., S. H. Doerr, K. Oostindie, A. K. Ziogas, and C. J. Ritsema. 2001. "Water repellency and critical soil water content in a dune sand." Soil Sci. Soc. Am. J. 65 (6): 1667–1674. https://doi.org/10.2136/sssaj2001.1667.
- Dennison, P. E., S. C. Brewer, J. D. Arnold, and M. A. Moritz. 2014. "Large wildfire trends in the western United States, 1984–2011." *Geophys. Res. Lett.* 41 (8): 2928–2933. https://doi.org/10.1002/2014GL059576.
- Doerr, S. H., R. A. Shakesby, and R. Walsh. 2000. "Soil water repellency: Its causes, characteristics and hydro-geomorphological significance." *Earth Sci. Rev.* 51 (1–4): 33–65. https://doi.org/10.1016/S0012-8252 (00)00011-8.
- Doerr, S. H., and A. D. Thomas. 2000. "The role of soil moisture in controlling water repellency: New evidence from forest soils in Portugal." J. Hydrol. 231–232 (May): 134–147. https://doi.org/10.1016/S0022 -1694(00)00190-6.
- Fourie, A. B., D. Rowe, and G. E. Blight. 1999. "The effect of infiltration on the stability of the slopes of a dry ash dump." *Géotechnique* 49 (1): 1–13. https://doi.org/10.1680/geot.1999.49.1.1.
- Gartner, J. E., S. H. Cannon, and P. M. Santi. 2014. "Empirical models for predicting volumes of sediment deposited by debris flows and sediment-laden floods in the transverse ranges of southern California." *Eng. Geol.* 176 (Jun): 45–56. https://doi.org/10.1016/j.enggeo.2014 .04.008.
- Gartner, J. E., S. H. Cannon, P. M. Santi, and V. G. Dewolfe. 2008. "Empirical models to predict the volumes of debris flows generated by recently burned basins in the western US." *Geomorphology* 96 (3–4): 339–354. https://doi.org/10.1016/j.geomorph.2007.02.033.
- Godt, J. W., R. L. Baum, and N. Lu. 2009. "Landsliding in partially saturated materials." *Geophys. Res. Lett.* 36 (2): 1–5. https://doi.org/10.1029/2008GL035996.
- Gray, D. H., and R. B. Sotir. 1996. *Biotechnical and soil bioengineering slope stabilization: A practical guide for erosion control.* New York: Wiley.
- Griffiths, D. V., and G. A. Fenton. 2004. "Probabilistic slope stability analysis by finite elements." J. Geotech. Geoenviron. Eng. 130 (5): 507. https://doi.org/10.1061/(ASCE)1090-0241(2004)130:5(507).
- Hammond, C. 1992. Vol. 285 of Level I stability analysis (LISA) documentation for version 2.0. Ogden, UT: USDA, Forest Service, Intermountain Research Station.
- Hazra, B., V. Gadi, A. Garg, C. W. W. Ng, and G. K. Das. 2017. "Probabilistic analysis of suction in homogeneously vegetated soils." *Catena* 149 (Feb): 394–401. https://doi.org/10.1016/j.catena.2016.10.014.
- Jha, S. K. 2015. "Effect of spatial variability of soil properties on slope reliability using random finite element and first order second moment methods." *Indian Geotech. J.* 45 (2): 145–155. https://doi.org/10.1007 /s40098-014-0118-2.
- Jiang, S. H., D. Q. Li, Z. J. Cao, C. B. Zhou, and K. K. Phoon. 2015. "Efficient system reliability analysis of slope stability in spatially variable soils using Monte Carlo simulation." J. Geotech. Geoenviron. Eng. 141 (2): 04014096. https://doi.org/10.1061/(ASCE)GT.1943-5606.0001227.
- King, P. M. 1981. "Comparison of methods for measuring severity of water repellence of sandy soils and assessment of some factors that affect its measurement." Soil Res. 19 (3): 275–285. https://doi.org/10.1071 /SR9810275.
- Lambe, T. W., and R. V. Whitman. 1969. Soil mechanics. New York: John Wiley and Sons.
- Lee, L. M., N. Gofar, and H. Rahardjo. 2009. "A simple model for preliminary evaluation of rainfall-induced slope instability." *Eng. Geol.* 108 (3–4): 272–285. https://doi.org/10.1016/j.enggeo.2009.06.011.
- Lu, N., and J. Godt. 2008. "Infinite slope stability under steady unsaturated seepage conditions." Water Resour. Res. 44 (11): W11404. https://doi .org/10.1029/2008WR006976.
- Lu, N., and W. J. Likos. 2006. "Suction stress characteristic curve for unsaturated soil." J. Geotech. Geoenviron. Eng. 132 (2): 131–142. https://doi.org/10.1061/(ASCE)1090-0241(2006)132:2(131).

- Masson-Delmotte, V., et al. 2021. "Climate change 2021: The physical science basis." In *Contribution of working group I to the sixth assessment report of the intergovernmental panel on climate change*. Cambridge, UK: Cambridge University Press.
- Megahan, W. F. 1983. "Hydrologic effects of clearcutting and wildfire on steep granitic slopes in Idaho." *Water Resour. Res.* 19 (3): 811–819. https://doi.org/10.1029/WR019i003p00811.
- Meyer, G. A., J. L. Pierce, S. H. Wood, and A. J. T. Jull. 2001. "Fire, storms, and erosional events in the Idaho batholith." *Hydrol. Processes* 15 (15): 3025–3038. https://doi.org/10.1002/hyp.389.
- Muntohar, A. S., and H. J. Liao. 2008. "Analysis of rainfall-induced infinite slope failure during typhoon using a hydrological–geotechnical model." *Environ. Geol.* 56 (6): 1145–1159. https://doi.org/10.1007/s00254-008 -1215-2.
- Ng, C. W. W., V. Kamchoom, and A. K. Leung. 2016. "Centrifuge modelling of the effects of root geometry on transpiration-induced suction and stability of vegetated slopes." *Landslides* 13 (5): 925–938. https://doi.org/10.1007/s10346-015-0645-7.
- Oorthuis, R., M. Hürlimann, A. Fraccica, A. Lloret, J. Moya, C. Puig-Polo, and J. Vaunat. 2018. "Monitoring of a full-scale embankment experiment regarding soil–vegetation–atmosphere interactions." *Water* 10 (6): 688. https://doi.org/10.3390/w10060688.
- Parise, M., and S. H. Cannon. 2012. "Wildfire impacts on the processes that generate debris flows in burned watersheds." *Nat. Hazards* 61 (1): 217–227. https://doi.org/10.1007/s11069-011-9769-9.
- Parsons, A., P. Robichaud, S. Lewis, C. Napper, and J. Clark. 2010. Field guide for mapping post-fire soil burn severity. General Technical Rep. No. RMRS-GTR-243. Berkeley, CA: USDA, Forest Service, Pacific Southwest Forest and Range Experiment Station.
- Philip, J. R. 1991. "Hillslope infiltration: Planar slopes." Water Resour. Res. 27 (1): 109–117. https://doi.org/10.1029/90WR01704.
- Phoon, K. K., A. Santoso, and S. T. Quek. 2010. "Probabilistic analysis of soil-water characteristic curves." J. Geotech. Geoenviron. Eng. 136 (3): 445–455. https://doi.org/10.1061/(ASCE)GT.1943-5606.0000222.
- Robichaud, P. R., J. L. Beyers, and D. G. Neary. 2000. Evaluating the effectiveness of postfire rehabilitation treatments. General Technical Rep. No. RMRS-GTR-63. Fort Collins, CO: USDA, Forest Service, Rocky Mountain Research Station.
- Scalia, J., IV, C. H. Benson, G. L. Bohnhoff, T. B. Edil, and C. D. Shackelford. 2014. "Long-term hydraulic conductivity of a bentonite-polymer composite permeated with aggressive inorganic solutions." J. Geotech. Geoenviron. Eng. 140 (3): 04013025. https://doi.org/10.1061/(ASCE)GT.1943-5606.0001040.
- Schmidt, K. M., J. J. Roering, J. D. Stock, W. E. Dietrich, D. R. Montgomery, and T. Schaub. 2001. "The variability of root cohesion as an influence on shallow landslide susceptibility in the Oregon Coast Range." Can. Geotech. J. 38 (5): 995–1024. https://doi.org/10.1139/t01-031.

- Sidle, R. C., and H. Ochiai. 2006. "Landslides processes, prediction, and land use." In Vol. 18 of *Water resources monograph*, 312. Washington, DC: American Geophysical Union.
- Smith, A. M., et al. 2016. "The science of firescapes: Achieving fire-resilient communities." *Bioscience* 66 (2): 130–146. https://doi.org/10.1093/biosci/biv182.
- Staley, D. M., J. W. Kean, S. H. Cannon, K. M. Schmidt, and J. L. Laber. 2013. "Objective definition of rainfall intensity—duration thresholds for the initiation of post-fire debris flows in southern California." *Land-slides* 10 (5): 547–562. https://doi.org/10.1007/s10346-012-0341-9.
- Staley, D. M., J. A. Negri, J. W. Kean, J. L. Laber, A. C. Tillery, and A. M. Youberg. 2016. Updated logistic regression equations for the calculation of post-fire debris-flow likelihood in the western United States. Reston, VA: US Department of the Interior, USGS.
- Staley, D. M., J. A. Negri, J. W. Kean, J. L. Laber, A. C. Tillery, and A. M. Youberg. 2017. "Prediction of spatially explicit rainfall intensity duration thresholds for post-fire debris-flow generation in the western United States." *Geomorphology* 278 (Feb): 149–162. https://doi.org/10 .1016/j.geomorph.2016.10.019.
- Swanson, F. J. 1981. "Fire and geomorphic processes." In *Fire regimes and ecosystem properties*, edited by H. A. Mooney, T. M. Bonnicksen, N. L. Christensen, J. E. Lotan, and W. A. Reiners, 401–444. Washington, DC: USDA.
- Terzaghi, K., and R. B. Peck. 1967. *Soil mechanics in engineering practice*. 2nd ed. New York: Wiley.
- Van Genuchten, M. T. 1980. "A closed-form equation for predicting the hydraulic conductivity of unsaturated soils." Soil Sci. Soc. Am. J. 44 (5): 892–898. https://doi.org/10.2136/sssaj1980.03615995004400 050002x.
- Van't Woudt, B. D. 1959. "Particle coatings affecting the wettability of soils." J. Geophys. Res. 64 (2): 263–267. https://doi.org/10.1029 /JZ064i002p00263.
- Westerling, A. L. 2016. "Increasing western US forest wildfire activity: Sensitivity to changes in the timing of spring." *Phil. Trans. R. Soc. B* 371 (Jun): 20150178. https://doi.org/10.1098/rstb.2015.0178.
- Westerling, A. L., H. G. Hidalgo, D. R. Cayan, and T. W. Swetnam. 2006. "Warming and earlier spring increase western US forest wildfire activity." *Science* 313 (5789): 940–943. https://doi.org/10.1126/science.1128834.
- Wondzell, S. M., and J. G. King. 2003. "Postfire erosional processes in the Pacific Northwest and Rocky Mountain regions." *For. Ecol. Manage*. 178 (1–2): 75–87. https://doi.org/10.1016/S0378-1127(03)00054-9.
- Wu, T. H., M. M. Riestenberg, and A. Flege. 1995. Root properties for design of slope stabilization. London: Thomas Telford.
- Zhao, Y., Y. Wang, and X. Zhang. 2021. "Spatial and temporal variation in soil bulk density and saturated hydraulic conductivity and its influencing factors along a 500 km transect." *Catena* 207 (Dec): 105592. https:// doi.org/10.1016/j.catena.2021.105592.